New Inorganic−Organic Hybrid: Synthesis and Structural Characterization of an Alumino(oxalato)phosphate

Nevenka Rajic,*[,†,‡] Natasa Zabukovec Logar,[†] Gregor Mali,[†] and Venceslav Kaucic[†,§]

National Institute of Chemistry, Ljubljana, Slovenia, Faculty of Technology and Metallurgy, University of Belgrade, Belgrade, Yugoslavia, and University of Ljubljana, Slovenia

Received October 30, 2002. Revised Manuscript Received December 16, 2002

A new 3-D alumino(oxalato)phosphate, $[H_3NCH(CH_3)CH_2NH_3]_2[Al_4P_6O_{20}(OH)_4(C_2O_4)(H_2O)]$, consists of aluminophosphate layers which are pillared by oxalate anions. It contains a hybrid 12-membered channel where guest species, diprotonated 1,2-diaminopropane and water molecules, are found. The layers are composed of AlO_6, AlO_4, and PO_4 polyhedra giving double chains, which are interconnected through Al−O−P−O−Al bridges. Oxalate ions are quadridentately bonded by participating in the coordination of AlO_6 and by bridging the aluminophosphate layers. The guest species strongly interact with the alumino(oxalato)-phosphate layers which is evidenced by solid-state NMR spectroscopy. Crystal data are: triclinic, space group $P\bar{1}$, $a = 8.611(1)$ Å, $b = 9.096(1)$ Å, $c = 11.371(1)$ Å, $\alpha = 104.811(1)°$, $\beta = 111.368(1)°$, and $\gamma = 94.248(1)°$, $V = 787.9(1)$ Å^3, and R = 0.041.

Introduction

Open-framework aluminophosphates (AlPOs) still represent a fertile field of investigation because of their enhanced structural and compositional diversity. The aluminophosphates obtained in the early synthetic efforts were strictly based on tetrahedral connectivity, with an Al/P ratio of unity. Different networks and framework structures were mainly obtained by using various organic species to act as structure-directing agents. Recently, a large number of AlPOs have appeared with an Al/P ratio of nonunity,[1−5] thus still extending the structural and compositional diversities. These solids are one-, two-, or three-dimensional, with a negatively charged framework in which protonated organic ammonium cations compensate the charge while interacting extensively with the inorganic host.

Introduction of species which possess a bridging functionality, such as the oxalate ions, offers a further opportunity in the creation of novel structural features in the AlPOs chemistry. Thus, an unusual layered aluminophosphate containing oxalate anions covalently bonded to the framework has recently been reported.[6] Unique structural properties of this inorganic−organic hybrid are manifested in a double AlO_6/HPO_4 chain and a bonding of oxalate groups which act as bidentate ligands to Al^{3+} and hold the structure together by strong interlayer P−O−H−oxalate hydrogen bonds. Also, a three-dimensional structure in which the linkages between the AlO_6 octahedra, PO_4 tetrahedra, and oxalate units lead to the formation of a large circular 12-membered channel is very similar to that of the naturally occurring aluminosilicate, gmelinite.[7] Finally, the "phosphate−oxalate" units have been shown to yield frameworks with many different metals.[8−14] Taking this into account, it seems likely that the combination of a relatively rigid inorganic framework with flexibile organic ligands could provide a new synthetic route to open-framework materials.

In this paper we report the synthesis and structural features of a new alumino(oxalato)-phosphate obtained in the presence of 1,2-diaminopropane (DAP), which contains not only the characteristic eight-membered rings but also unique hybrid 12-membered rings.

Experimental Section

The synthesis was carried out hydrothermally. Aluminum isopropoxide (APRO), H_3PO_4, oxalic acid dihydrate (ox), DAP, and water were used in the molar ratio 1:6:1:2:100, respectively. APRO was added slowly to half of the required amount

* To whom correspondence should be addressed. Fax: +386-1-4760-300. E-mail: nevenka.rajic@ki.si.
† National Institute of Chemistry.
‡ University of Belgrade.
§ University of Ljubljana.

(1) Yu, J.; Xu, R.; Li, J. *Solid State Sci.* **2000**, *2*, 181.
(2) Yu, J.; Xu, R.; Li, J. *Microporous Mesoporous Mater.* **2001**, *48*, 47.
(3) Marichal, C.; Vidal, L.; Delmotte, L.; Patarin, J. *Microporous Mesoporous Mater.* **2000**, *34*, 149.
(4) Tuel, A.; Gramlich, V.; Baerlocher, Ch. *Microporous Mesoporous Mater.* **2001**, *46*, 57.
(5) Tuel, A.; Gramlich, V.; Baerlocher, Ch. *Microporous Mesoporous Mater.* **2001**, *47*, 217.
(6) Lightfoot, P.; Lethbridge, Z. A. D.; Morris, R. E.; Wragg, D. S.; Wright, P. A. *J. Solid State Chem.* **1999**, *143*, 74.
(7) Kedarnath, K.; Choudhury, A.; Natarajan, S. *J. Solid State Chem.* **2000**, *150*, 324.
(8) Choudhury, A.; Natarajan, S.; Rao, C. N. R. *Chem. Eur. J.* **2000**, *6*, 1168.
(9) Natarajan, S. *Solid State Sci.* **2002**, *10*, 1331, and references therein.
(10) Choudhury, A.; Natarajan, S. *Solid State Sci.* **2002**, *2*, 365.
(11) Neeraj, S.; Natarajan, S.; Rao, C. N. R. *J. Chem. Soc., Dalton Trans.* **2001**, 289.
(12) Lethbridge, Z. A. D.; Hillier, A. D.; Cywinski, R.; Lightfoot, P. *J. Chem. Soc., Dalton Trans.* **2000**, 1595, and references therein.
(13) Rao, C. N. R.; Natarajan, S.; Choudhury, A.; Neeraj, S.; Vaidhyanathan, R. *Acta Cryst. B* **2001**, *57*, 1.
(14) Prasad, P. A.; Neeraj, S.; Vaidhyanathan, R.; Natarajan, S. *J. Solid State Chem.* **2002**, *166*, 128.

10.1021/cm021343u CCC: $25.00
Published on Web 03/22/2003

Table 1. Crystallographic Data for the Single X-ray Diffraction Study of the Alumino(oxalato)phosphate

formula of asymmetric unit	$Al_2P_3O_{14.415}N_2C_4H_{14}$
crystal system	triclinic
a (Å)	8.611(1)
b (Å)	9.096(1)
c (Å)	11.371(1)
α (°)	104.811(1)
β (°)	111.368(1)
γ (°)	94.248(1)
V (Å^3)	787.9(1)
space group	$P\bar{1}$
D_c (g·cm^{-3})	1.977
T (°C)	20(1)
λ(Mo Kα) (Å)	0.71073
hkl-data limits	$-11 \le h \le 10$, $-11 \le k \le 11$, $-14 \le l \le 14$
total data	6247
unique reflections	3571
observed data ($F^2 \ge 2\sigma(F^2)$)	2942
R_{int}	0.027
refined data	2942
parameters	292
R (on F)	0.041
R_w (on F)	0.039
$\Delta\rho_{max}$ (e Å^{-3})	0.658
$\Delta\rho_{min}$ (e Å^{-3})	−0.971

of water and the mixture was stirred for 5 min using an Ultra-Turrax mixer (Janke and Kunkel, GmbH). To this suspension H_3PO_4 was added dropwise followed by a solution of ox (dissolved in the remaining amount of water). Finally, DAP was added dropwise to the resulting solution and stirred for at least 10 min. The final pH was about 2 and did not change throughout the hydrothermal crystallization. The crystallization performed in a Teflon-lined stainless steel autoclave at 130 °C for 4 days yielded a white crystalline product. It was separated from the mother liquor by decantation, washed with distilled water, treated by ultrasonification, and finally dried in air.

Aluminum and phosphorus were analyzed by inductively coupled plasma emission spectroscopy. Carbon, hydrogen and nitrogen were determined with a standard C,H,N analyzer. (Found: C, 10.2; N, 6.2; H, 4.5; Al, 11.2; P, 20.1 wt %).

The crystal morphology and size were analyzed by using a JEOL 5800 SEM. Fourier transform infrared (FTIR) spectra were collected on a Digilab-FTS-80 spectrophotometer. The spectra were recorded from 4000 to 400 cm^{-1}, using the KBr wafer technique. Thermogravimetric analyses and differential scanning calorimetry (TGA and DSC) were performed using a SDT 2960 simultaneous DSC-TGA instrument (TA Instruments) at a heating rate of 10 °C/min under a helium flow.

A colorless prismatic-like single crystal (0.225 × 0.045 × 0.038 mm^3) was selected for the structural analysis. The intensity data were collected on a Nonius Kappa CCD diffractometer by using the Mo Kα radiation. Unit cell parameters were determined by least-squares refinement on the basis of 3290 reflections. The structure was solved combining the SIR97 program package[15] and Fourier maps calculation using the Xtal 3.4 program package.[16] The latter was also used for the structure refinement and the interpretation. The hydrogen atoms were located from the difference Fourier maps and were isotropically refined. All non-hydrogen atoms were anisotropically refined. A brief summary of the crystallographic data is given in Table 1. Final atomic parameters with selected bond and contact distances are presented in Tables 2 and 3, respectively.

Solid-state NMR measurements were performed on a narrow-bore Varian Unity Inova spectrometer operating at 150.87, 242.89, and 600.03 MHz for ^{13}C, ^{31}P, and ^{1}H nuclei, respectively. A Doty triple-tuned CPMAS probehead was used. The sample was spun at a spinning rate of 10 kHz. The carbon and phosphorus NMR spectra were referenced to carbon and phosphorus resonances in tetramethylsilane and 85 wt % H_3PO_4, respectively.

Table 2. Fractional Atomic Coordinates and Equivalent Displacement Parameters (Å^2)[a]

	x	y	z	U_{eq}
P(1)	0.17090(9)	0.48318(8)	0.18037(7)	0.0139(2)
P(2)	0.22918(9)	0.46388(8)	0.66575(7)	0.0134(2)
P(3)	0.14070(10)	0.00776(9)	−0.20976(9)	0.0223(3)
AL(1)	0.04841(11)	0.32627(10)	0.35600(8)	0.0155(3)
AL(2)	0.17332(10)	0.36380(9)	−0.10345(8)	0.0123(3)
O(1)	0.1904(2)	0.3684(2)	0.0657(2)	0.0157(7)
O(2)	0.0261(3)	0.5667(2)	0.1378(2)	0.0205(8)
O(3)	0.3325(3)	0.6120(3)	0.2576(2)	0.0265(9)
O(4)	0.1553(3)	0.3956(3)	0.2742(2)	0.0294(9)
O(5)	0.4180(2)	0.5225(2)	0.7338(2)	0.0213(8)
O(6)	0.1795(3)	0.3693(3)	0.5206(2)	0.0228(8)
O(7)	0.1679(3)	0.3572(2)	−0.2698(2)	0.0192(7)
O(8)	−0.1395(3)	0.3956(2)	0.3312(2)	0.0245(8)
O(9)	0.0766(2)	0.1540(2)	−0.1656(2)	0.0175(7)
O(10)	0.0129(3)	0.1244(2)	0.2921(2)	0.0280(8)
O(11)	0.2250(5)	0.0335(4)	−0.3061(4)	0.0699(16)
O(12)	0.2672(3)	−0.0331(3)	−0.0990(3)	0.0445(11)
O(13)	0.4088(2)	0.3068(2)	−0.0573(2)	0.0155(7)
O(14)	0.3162(2)	0.5759(2)	−0.0260(2)	0.0151(7)
O(15)	0.1288(14)	−0.1083(15)	0.4583(9)	0.088(7)[b]
C(1)	0.5263(3)	0.4219(3)	−0.0092(3)	0.0135(9)
C(2)	0.3538(6)	−0.0636(5)	0.2188(5)	0.0460(18)
C(3)	0.3799(5)	0.1105(4)	0.2481(4)	0.0368(16)
C(4)	0.4862(9)	0.1900(6)	0.3930(5)	0.061(3)
N(1)	0.2141(5)	−0.1483(4)	0.0895(5)	0.0438(16)
N(2)	0.4639(4)	0.1607(4)	0.1671(3)	0.0260(11)
H(1)	0.403(8)	0.581(7)	0.265(6)	0.07(2)
H(2)	0.177(14)	−0.038(11)	−0.371(9)	0.18(5)
H(3)	0.227(6)	−0.103(6)	0.024(5)	0.056(14)
H(4)	0.225(7)	−0.239(7)	0.063(5)	0.057(15)
H(5)	0.125(9)	−0.150(8)	0.102(7)	0.10(2)
H(6)	0.557(5)	0.125(4)	0.175(4)	0.026(10)
H(7)	0.393(7)	0.125(6)	0.077(6)	0.063(15)
H(8)	0.494(5)	0.263(5)	0.197(4)	0.029(10)
H(9)	0.322(6)	−0.089(6)	0.289(5)	0.060(15)
H(10)	0.453(6)	−0.099(6)	0.217(5)	0.051(13)
H(11)	0.270(6)	0.142(5)	0.221(5)	0.049(13)
H(12)	0.507(6)	0.304(6)	0.421(5)	0.050(13)
H(13)	0.421(7)	0.172(7)	0.442(6)	0.068(16)
H(14)	0.606(8)	0.166(7)	0.423(6)	0.069(17)

[a] $U_{eq} = (1/3)\sum_i\sum_j U_{ij} a_i \cdot a_j \cdot a_i a_j$. [b] The refined occupancy is 0.416(17).

Table 3. Selected Bond and Contact Distances (Å)

P(1)−O(1)	1.520(2)	P(2)−O(5)	1.507(2)
P(1)−O(2)	1.502(2)	P(2)−O(6)	1.534(2)
P(1)−O(3)	1.556(2)	P(2)−O(7)	1.525(3)
P(1)−O(4)	1.521(3)	P(2)−O(8)	1.541(2)
P(3)−O(9)	1.515(2)	Al(1)−O(4)	1.717(3)
P(3)−O(10)	1.535(2)	Al(1)−O(6)	1.717(2)
P(3)−O(11)	1.571(5)	Al(1)−O(8)	1.734(3)
P(3)−O(12)	1.487(3)	Al(1)−O(10)	1.751(2)
Al(2)−O(1)	1.864(3)	Al(2)−O(9)	1.866(2)
Al(2)−O(2)	1.817(2)	Al(2)−O(13)	2.043(2)
Al(2)−O(7)	1.860(3)	Al(2)−O(14)	2.000(2)
O(13)−C(1)	1.251(3)	O(14)−C(1)	1.264(3)
C(1)−C(1)	1.510(4)		
C(2)−C(3)	1.514(6)	C(2)−N(1)	1.482(5)
C(3)−C(4)	1.506(6)	C(3)−N(2)	1.494(7)
N(1)···O(14)	2.877(5)	N(1)···O(12)	2.774(7)
N(1)···O(9)	2.932(6)	N(2)···O(5)	2.771(4)
N(2)···O(12)	2.925(5)	N(2)···O(12)	2.868(4)
O(15)···O(11)	2.45(1)	O(15)···O(7)	2.99(1)
O(15)···O(9)	3.045(9)	O(15)···O(10)	3.17(1)
O(15)···O(11)	3.13(1)		

Results and Discussion

SEM analysis shows that the colorless as-synthesized material is composed of aggregates as well as prism-like single crystals, as illustrated in Figure 1. The FTIR

(15) Altomare, A.; Burla, M. C.; Camalli, M.; Cascarano, G.; Giacovazzo, C.; Guagliardi, A.; Maliterni, A. G. G.; Polidori, G.; Spagna, R. *J. Appl. Crystallogr.* **1999**, *32*, 115.

(16) Hall, S. R.; King, G. S. D.; Srewart, J. M. *Xtal 3.4. Users Manual*; University of Western Australia, 1997.

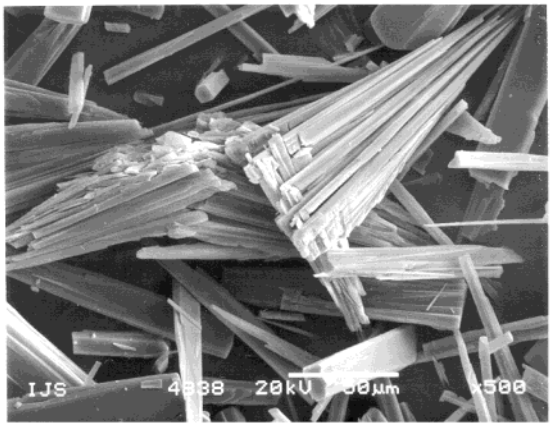

Figure 1. SEM photo of the alumino(oxalato)phosphate.

spectrum (Figure 2) displays bands characteristic of oxalate vibrations [ν_a(C═O) ∼ 1700 cm^{-1}] and a protonated amine [δ_d(NH_3^+) ∼ 1520 cm^{-1}], thus showing the presence of an organic component.

The results of TG and DSC analyses are given in Figure 3. The TG curve consists of three distinct parts. The first one takes place in a wide temperature range, which nears completion at ca. 300 °C (∼2% weight loss). The second weight loss occurs at 300−370 °C (∼6% weight loss), and the last one is completed up to 600 °C (16.5% weight loss). It seems that the first loss is thermally insignificant because only the other two are accompanied by the effects on the DSC curve. Namely, up to 600 °C there are two endotherms: at 367 and 385 °C. According to the elemental analysis, the first thermal event (up to 300 °C) corresponds to desorption of one water molecule, while the other two could be attributed to a decarbonylation process (calc. for 2 CO is ca. 6%) and the decomposition of DAP species (calc. for 2 DAP is ca. 16%), respectively. Taking into account these results, an overall chemical formula of the obtained product can be as follows:

$$(H_2DAP)_2^{4+}\cdot[Al_4P_6O_{20}(OH)_4(C_2O_4)]^{4-}\cdot(H_2O)$$

The single-crystal X-ray analysis confirms the formula. The compound crystallizes in the triclinic space group $P\bar{1}$ with the lattice parameters a = 8.611(1) Å, b = 9.096(1) Å, c = 11.371(1) Å, α = 104.811(1)°, β = 111.368(1)°, and γ = 94.248(1)°. The structure consists of an open-framework macroanion $[Al_4P_6O_{20}(OH)_4(C_2O_4)]^{4-}$ (Figure 4). Each asymmetric unit contains two crystallographically distinct Al atoms and three P atoms (Figure 5). Al(1) is tetrahedrally coordinated and shares four oxygens with the adjacent P atoms. The Al(1)−O bond lengths are in the range of 1.717(2) Å to 1.751(2) Å. Al(2) is octahedrally coordinated and shares four oxygens with P atoms, while the remaining two vertexes belong to an oxalate group. The Al(2)−O bond lengths vary within the range of 1.817(2) Å to 2.043(2) Å. The three crystallographically distinct P atoms are tetrahedrally coordinated. Two of them each have three oxygen atoms bridging to the adjacent Al atoms (their P−O bond lengths vary within the range of 1.502(2) Å to 1.556(2) Å), the remaining vertex being P(1)−OH (1.556(2) Å) or P(2)═O (1.507(2) Å). P(3) shares two oxygens with the adjacent Al atoms (the P−O bond lengths are 1.515(2) Å and 1.535(2) Å, respectively), the

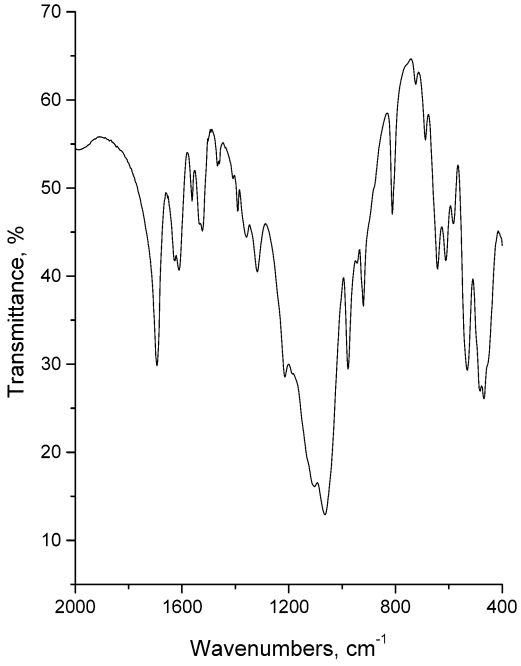

Figure 2. FTIR spectrum of the alumino(oxalato)phosphate.

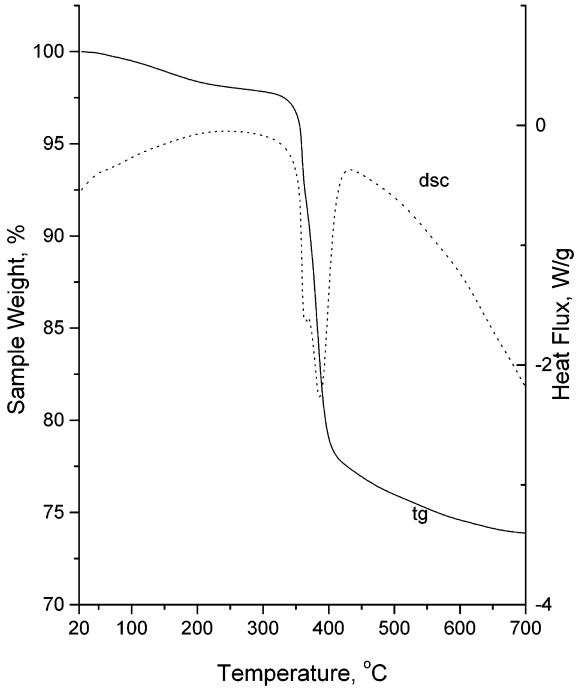

Figure 3. TG/DSC curves.

remaining vertexes being P═O (1.487(3) Å) and P−OH (1.571(5) Å) groups (Table 3).

The framework consists of aluminophosphate layers with characteristic eight-membered ring channels as shown in Figure 6. It can be seen that the connectivity between $P(1)O_4$, $P(2)O_4$, $Al(1)O_4$, and $Al(2)O_6$ polyhedra also results in double chains which are interconnected through the Al(1)−O−P(3)−O−Al(2) bridges. Oxalate units participate in the coordination of Al(2) atoms. They are quadridentately bonded as they bridge the aluminophosphate layers. As a comparison, oxalate units exhibit the bidentate coordination mode in the alumino(oxalate)phosphate layered structure obtained in the presence of 1,2-diaminoethane.[6]

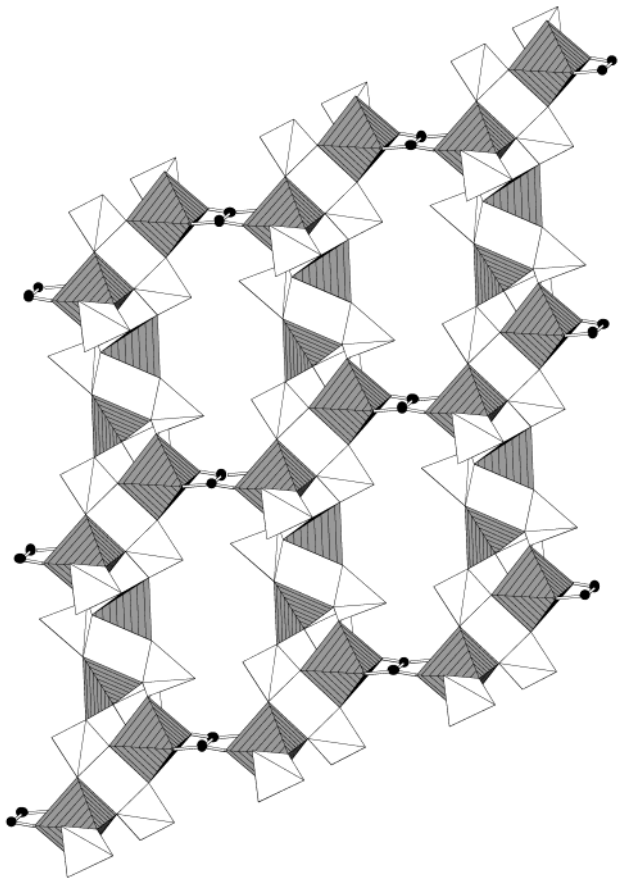

Figure 4. Polyhedral schematic presentation of alumino(oxalato)phosphate layers, which are connected through oxalate bridges (C-atoms are shown as circles) in a three-dimensional framework structure. A [010] projection shows characteristic 12-member ring channels (PO_4 tetrahedra are white, AlO_4 tetrahedra and AlO_6 octahedra are gray). The view is parallel to the aluminophosphate layers.

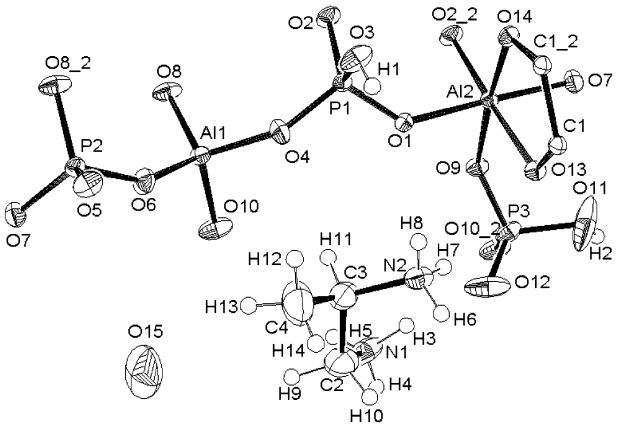

Figure 5. Asymmetric unit with the full coordination environments of the P and Al atoms. Thermal ellipsoids are given at 50% probability. The oxalate unit is located on a crystallographic inversion center.

The connectivity between the aluminophosphate layers and the oxalate units yields a 3D architecture giving rise to a hybrid 12-membered ring channel. It is worth noticing that the gmelinite-like alumino(oxalato)phosphate is also characterized by 12-membered channels.[7] In contrast to the present structure, the latter channels are formed by double six-rings. However, in both structures the oxalate units are bonded similarly – in the bidentate manner. This clearly shows that organic ligands with a bonding flexibility, such as oxalate units, can significantly expand structural specificity and diversity of aluminophosphates.

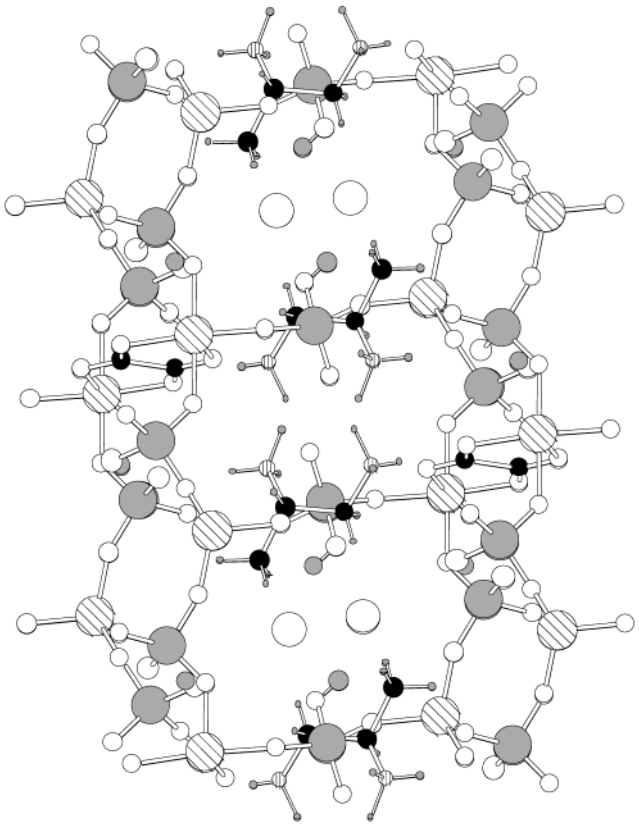

Figure 6. Alumino(oxalato)phosphate structure in [100] direction with the eight-membered ring channels and the position of template 1,2-diaminopropane, and water molecules in the structure (P, big gray circles; Al, big hatched circles; O, white circles; C, black circles; N, small hatched circles; H, small gray circles). The view is perpendicular to the aluminophosphate layer.

Diprotonated DAP and water molecules occupy the 12-membered ring. Their positions are shown in Figure 6. Both are in a strong interaction with the aluminophosphate layers by hydrogen bonding. Thus, the shortest distance between an ammine group and a bridging oxygen [such as N(1)···O(9)] is 2.932(6) Å. The second nitrogen atom participates in two hydrogen bonds to the terminal oxygen atoms as characterized by N(2)···O(5) and N(2)···O(12) distances of 2.771(4) and 2.868(4) Å, respectively. The shortest distance between a water molecule and the hydroxyl group attached to the P(3) atom [O(15)···O(11)] is 2.45(1) Å indicating also the presence of a strong hydrogen bond. Finally, DAP interacts also with oxalate units via hydrogen bonds as can be concluded from the N(1)···O(14) distance of 2.877(5) Å (Table 3). The latter could be used as an explanation for the deoxalation process, which proceeds via liberation of CO during the thermal degradation (vide supra). Namely, the thermal decomposition of most oxalate complexes takes place with the formation of basic carbonates by evolving CO and CO_2.[17,18]

Interactions of the template species with the host framework were also studied by the $^1H \rightarrow {}^{13}C$ CP MAS NMR spectroscopy. The spectrum is shown in Figure 7. Besides a narrow resonance line at 168 ppm belonging

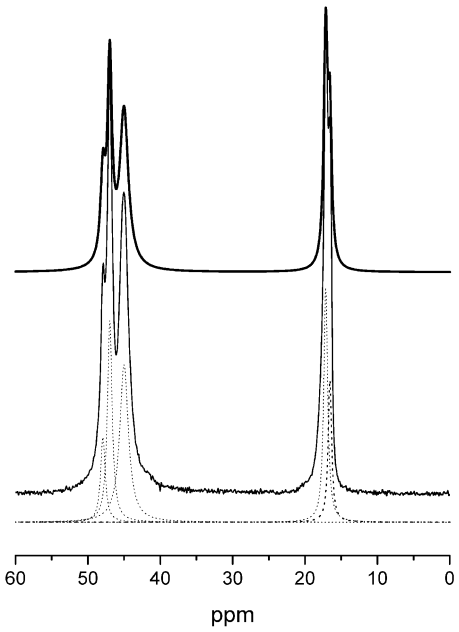

Figure 7. $^{1}H \rightarrow ^{13}C$ CPMAS NMR spectrum. The measured carbon spectrum, individual lines in the decomposition of the spectrum (dot), and the sum of decomposed lines (bold line). Only the part of the spectrum belonging to the carbon atoms from doubly protonated 1,2-diaminopropane is shown.

to the carbon nuclei of the oxalate groups (not shown) there are three main signals at 47, 45, and 17 ppm which can be assigned to the carbon nuclei in CH_2NH_3, $CHNH_3$, and CH_3 groups, respectively. It is evident that the signals belonging to the CH_2NH_3 and CH_3 groups are each split into two resonance lines (at 47.9 and 47 ppm in the ratio 68:32, and at 17.1 and 16.6 ppm in the ratio 65:35) indicating a disorder of DAP species. The analysis of both split carbon lines gives the ratio of occupancies of 2:1 indicating the presence of two conformations of the $CH_2CH(CH_3)$ fragment. It should be added that the X-ray analysis did not give a very clear-cut evidence for the disorder. However, examination of the final Fourier difference map revealed the presence of a weak electron density approximately 1.6 Å from the C(2) atom, which could be attributed to the presence of a partly occupied CH_3 group.

Because the DAP species is located close to the Al(1)−O−P(3)−O−Al(2) bridge, it seems likely that the disorder of DAP has an influence on the local environment of the P(3) site. ^{31}P MAS NMR spectrum (Figure 8) shows five peaks at −20.6, −18.4, −12.1, −8.9, and −2.7 ppm. The intensities of the first two and the sum of the remaining three are equal, suggesting that the last three peaks belong to the phosphorus nuclei occupying crystallographically equivalent but magnetically inequivalent sites such as the P(3) site. It is worth noticing that the precise assignment of NMR signals to the three crystallographically distinct sites has been accomplished by the $^{27}Al-^{31}P$ double resonance NMR measurements which was discussed in detail in our previous paper.[19]

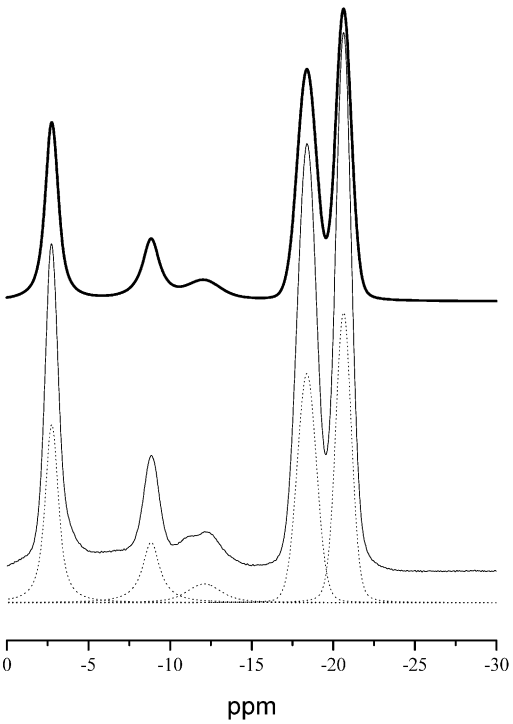

Figure 8. ^{31}P MAS NMR spectrum. The measured phosphorus spectrum, individual lines in the decomposition of the phosphorus spectrum (dot), and the sum of decomposed lines (bold line).

However, three resonances instead of the expected two indicate that not only the DAP species but also some other one has an influence on the P(3) site. The short distance between the hydroxyl group attached to the P(3) and the oxygen atom from the water molecule as well as a detailed NMR investigation[19] show that the water molecule also affects the P(3). The ratio of intensities of the last two resonances is about 2:1, which is in accordance with the ratio of occupancies of the two DAP conformers. Finally, the fact that the P(3) atoms are influenced by the guest species finds an additional support in the values of the temperature factor for P(3). They are more than two times larger than those for P(1) and P(2).

Acknowledgment. Financial support by Ministry of Education, Science and Sport, Republic of Slovenia, is gratefully acknowledged (Grant P0-0516-0104). We thank Amalija Golobič for the X-ray CCD data collection.

Note Added after Print Publication

The CIF file for this article was not made available to the reader when the article was originally published on the Web 03/22/2003 (ASAP) and in the April 22, 2003 issue (Vol. 15, No. 8, pp 1734−1738). The correct electronic version of the paper was published on 08/19/2003 and an Addition and Correction appears in the September 23, 2003 issue (Vol. 15, No. 19).

Supporting Information Available: Crystallographic data (CIF). This material is available free of charge via the Internet at http://pubs.acs.org.

CM021343U

(17) Foster, K. A.; House, J. E., Jr. *Thermochim. Acta* **1983**, *60*, 389.
(18) House, J. E., Jr.; Blumthal, T. G. *Thermochim. Acta* **1981**, *43*, 237.
(19) Mali, G.; Rajic, N.; Zabukovec Logar, N.; Kaucic, V. *J. Phys. Chem. B* **2003**, *107*, 1286.